International Journal of Rotating Machinery

WILEY

RESEARCH ARTICLE OPEN ACCESS

Prediction and Optimization of Turbine Blade Cooling Hole Configuration for Advanced Power Generation Gas Turbine Using Response Surface Methodology

S. Mohd Yunus[1,2] | A. Manap[1,3] | M. H. Ujir[4] | M. Satgunam[1] | N. Mohd Afandi[1] | F. Arith[5]

[1]Department of Mechanical Engineering, College of Engineering, Universiti Tenaga Nasional, Kajang, Selangor, Malaysia | [2]Materials Engineering and Testing Group, TNB Research Sdn Bhd, Kawasan Institusi Penyelidikan, Kajang, Selangor, Malaysia | [3]Institute of Sustainable Energy, Universiti Tenaga Nasional, Kajang, Selangor, Malaysia | [4]Power Plant Optimization Group, TNB Research Sdn Bhd, Kawasan Institusi Penyelidikan, Kajang, Selangor, Malaysia | [5]Faculty of Electronics and Computer Technology and Engineering, Universiti Teknikal Malaysia Melaka, Durian Tunggal, Malacca, Malaysia

Correspondence: S. Mohd Yunus (salmi.yunus@tnb.com.my)

Received: 8 September 2025 | **Revised:** 3 February 2026 | **Accepted:** 2 March 2026

Academic Editor: Phillip Ligrani

Keywords: advanced gas turbine | cooling hole configuration | fluid-structure interaction | response surface methodology | turbine blade

ABSTRACT

Advanced gas turbines play a crucial role in power generation, operating at turbine inlet temperatures exceeding 1200°C to maximize efficiency and output. While nickel-based superalloys provide structural integrity, their performance is limited at temperatures above 1250°C, necessitating the use of advanced cooling strategies. This study employs response surface methodology (RSM) to systematically analyze and optimize cooling hole configurations, enhancing thermal management in high-temperature environments. Existing configurations prove inadequate for next-generation gas turbines operating at 1400°C with cooling air at 400°C. Through predictive modeling, an optimal configuration is identified, characterized by a blade height of 300 mm, 45 holes with a diameter of 2.0 mm, and a spacing of 4.75 mm, which effectively reduces metal temperatures to below 1250°C. This optimized design significantly improves cooling efficiency and mitigates thermal hotspots, offering a viable solution for high-temperature turbine applications. The findings from this study offer a practical and scalable solution for thermal management in high-performance gas turbines, supporting the advancement of turbine technology capable of operating under more demanding thermal conditions.

1 | Introduction

Gas turbines (GTs) are fundamental to power generation, aerospace propulsion, and marine applications due to their high power-to-weight ratio, thermal efficiency, and operational reliability. In modern heavy-duty GTs used for power production, turbine inlet temperatures (TITs) have escalated to as high as 1600°C to meet growing efficiency demands and emission reduction targets [1]. However, turbine components fabricated from nickel (Ni)-based superalloys typically have an upper-temperature limit of approximately 1250°C, creating a significant thermal challenge [2]. Three core technologies have been developed to bridge this gap and ensure the longevity of turbine components: advanced superalloys, thermal barrier coatings (TBCs), and sophisticated cooling techniques. Among these, cooling systems play a pivotal role by directly mitigating thermal loads on turbine blades, ensuring safe operation under extreme conditions.

Cooling in GTs is primarily achieved by diverting high-pressure air from the compressor stage and channeling it through internal cooling passages and film cooling holes along the blade surface. This airflow forms an insulating film that reduces the external temperature exposure, protecting the blade from thermal degradation. Various strategies, including jet impingement, rib turbulators, and pin-fin arrays, are employed to enhance internal heat transfer, while film cooling ensures protection of the external surface.

Despite the availability of such techniques, cooling strategies remain highly proprietary and differ significantly among original equipment manufacturers (OEMs) [3]. Hybrid protection systems that combine internal and external cooling with TBCs have been implemented to enhance cooling effectiveness while maintaining aerodynamic performance. These systems enable safe operation at TITs up to 1400°C but require meticulous optimization of cooling hole geometry, specifically the cooling hole diameter, its arrangement, and spacing between holes, to strike a balance between thermal protection and structural efficiency. The cooling effectiveness is calculated using Equation (1) below [4]:

$$\text{Cooling effectiveness, } \varepsilon = \frac{T_g - T_{m,\max}}{T_g - T_{c,\text{in}}}, \qquad (1)$$

where ε is the cooling effectiveness, T_g is the hot gas temperature, $T_{m,\max}$ is the maximum blade metal surface temperature, and $T_{c,\text{in}}$ is the inlet cooling air temperature.

Recent research has investigated the impact of cooling hole geometries on film cooling effectiveness (ε), offering valuable insights and identifying several limitations. Table 1 compiles available cooling hole configurations and their respective limitations. The data in the table show the geometric arrangement, size, and shape, as well as the resultant temperature profiles in high-temperature environments, such as those encountered in GTs. For instance, Cai et al. [20] showed that staggered, multirow cooling configurations on the pressure side and near the blade tip effectively reduced local thermal hotspots. Du et al. [7] highlighted the role of internal cooling in complementing film cooling, particularly near the leading-edge stagnation zone. However, many studies are limited to simplified assumptions, such as using flat blade geometries, and fail to capture the complex aerothermal and structural behavior in actual turbine blades, thereby diminishing their applicability in real-world scenarios [21].

To address these challenges, optimization approaches are essential for efficiently analyzing the complex, nonlinear relationships between multiple design parameters and cooling performance. Response surface methodology (RSM) provides a computationally and statistically framework for early-stage optimization, surpassing available techniques such as genetic algorithms, particle swarm optimization, and machine learning. RSM constructs surrogate models that approximate the

TABLE 1 | Compilation of the available cooling hole configuration for the turbine blade.

Shape of hole	Injection angle from surface, °	Hole size, mm	Blade height, mm	No. of holes at LE/no. of row	TBC	$T_{\text{hot gas}}$, °C	T_{coolant}, °C	$T_{m,\max}$, °C	ε	Reference
○	60	2.0	77.2	10/1	✓	428	320	402	0.07[a]	Shi et al. [5]
○	—	2.0	180.0	60/3	×	1427	327	1287	0.13[a]	Abdelmaksoud & Wang [6]
○	—	2.0	76.2	32/4	×	1689	327	—	0.14	Du et al. [7]
○	45	—	200.0	—	×	34	22	—	0.10	Singh et al. [8]
○	43	3.0	300.0	20/1	×	30	15	—	0.88	Jiang et al. [9]
○	30	0.8	80.0	10/1	×	35	45	—	0.25	Zhang et al. [10]
○	25	6.35	254.0	16/2	×	25	—	—	0.35	Liu et al. [11]
⬡	—	0.5	64.0	—	×	100	20	—	0.05	Kim et al. [12]
○	30	4.5	77.2	52/3	✓	545	141	507	0.09[a]	Shi et al. [13]
○	45	2.0	76.2	32/1	✓	417	244	—	0.60	Zhang et al. [14]
○	30	6.4	—	28/1	×	43	23	40	0.05[a]	Wen et al. [15]
○	30	6.4	—	14/1	×	43	23	39	0.2[a]	
□	90	2.9	—	17/1	×	1400	500	—	0.487	Huang et al. [16]
○	5	4.8	200.0	39/1	×	227	20	—	0.62	Effendy et al. [17]
○	35	12.7	—	—	×	27	−23	—	0.18	Wang et al. [18]
○	35	—	114	22/1	×	—	—	—	0.6	Zhang et al. [19]

[a] ε is not provided by the author; thus, it was calculated using Equation (1).

interactions among variables, enabling rapid exploration of design spaces. In turbine cooling applications, RSM has been employed to assess the effects of hole geometry on metal temperature and ε [4, 22]. Li et al. [4] demonstrated that integrating RSM with conjugate heat transfer (CHT) simulations allowed for accurate predictions of cooling effectiveness. Wang et al. [18] used RSM to optimize shaped holes considering turbulence effects. Nevertheless, few investigations incorporate structural considerations to couple RSM with fluid-structure interaction (FSI) simulations to jointly optimize thermal performance and mechanical stability.

This study applies RSM in turbine blade cooling optimization through a comprehensive and integrative approach. Unlike prior work focusing solely on thermal performance, this research couples RSM with computational fluid dynamics (CFD) and FSI simulations to evaluate cooling effectiveness and structural integrity concurrently. This integrated framework ensures that optimized configurations enhance thermal management and maintain mechanical stability under operational loads. A key innovation involves systematically exploring the cooling hole diameter, spacing between holes, and the cooling hole arrangement, parameters that interact nonlinearly and influence blade temperatures. By employing RSM, the study efficiently identifies optimal configurations that minimize maximum blade temperature while adhering to material constraints. Cooling effectiveness serves as an intermediate thermal metric and does not directly indicate whether the blade remains within safe operating temperatures, as served by the thermal profile. Due to the increasing demands on turbine components in high-TIT environments, this work presents a validated optimization strategy that integrates statistical modeling with simulation tools.

2 | Methodology

The Box–Behnken design (BBD) was used to select the design points for computational analysis, and the main effects of the shape parameters were analyzed using analysis of variance (ANOVA). Subsequently, RSM was used to determine the optimal design variable to achieve the objective function generated and get $T_{m,\max}$ below 1250°C.

2.1 | Initialization of Population From Existing Cooling Hole Configurations

The initial step involves selecting candidate cooling hole designs from the existing literature to form a population for optimization, focusing on three key parameters: hole size, spacing, and blade height, each of which significantly influences coolant flow, temperature distribution, and thermal management. Hole size affects heat extraction efficiency, spacing determines coolant coverage, and blade height influences overall cooling performance. Equation (2) provides a method for calculating hole spacing along the leading edge (LE). To maintain structural integrity and keep turbine blade temperatures below the 1250°C operating limit for Ni-based superalloys, only the configurations with $\varepsilon > 0.375$ from Table 2 were selected. These configurations, summarized in Table 2, were then used to develop a predictive RSM model to guide design modifications and ensure that $T_{m,\max}$ stays below the critical threshold:

$$s_x = \frac{H}{n} - d, \tag{2}$$

where s_x is the spacing between holes in a spanwise direction (mm), H is the blade height (mm), and n is the number of holes.

TABLE 2 | Details cooling hole configurations with $\varepsilon > 0.375$.

ε	Hole size, mm	Blade height, mm	No. of hole at LE	s_x, mm
0.88	3.0	300.0	20	24.5
0.68	1.0	6.8	8	0.56
0.62	4.8	200.0	39	5.0
0.60	2.0	76.2	32	4.4
0.55	1.0	6.8	8	0.56

The row number of cooling holes has also been attributed to the film-cooling effectiveness. Abdelmaksoud and Wang [18] identified a lack of coolant discharge at the third row due to recirculation after the second row, hindering effective cooling. Similarly, Wen et al. [15] observed that a three-row cooling hole configuration outperformed a five-row setup in ε, challenging the assumption that more rows improve performance. Zhang et al. [14] highlighted that increasing the number of cooling rows leads to higher aerodynamic losses and increased coolant demand, thereby reducing overall turbine efficiency. Meanwhile, Zhang et al. [19] highlighted that film lift-off occurs after the second row degrades cooling efficiency. Singh et al. [8] and Shi et al. [13] emphasized the critical role of coolant temperature, showing that insufficiently cool coolant reduces heat transfer and ε. Du et al. [7] found that coolant near the stagnation line offers superior heat removal, with a decline in ε downstream, suggesting that both coolant temperature and internal cooling design significantly affect overall blade cooling performance. Therefore, this study is limited to a two-row arrangement. The holes are arranged in a staggered two-row pattern.

An investigation was conducted to evaluate various cooling hole arrangements, utilizing configurations from existing literature detailed in Table 2, which lists cooling hole configurations with the ε exceeding 0.375. According to Equation (1), ε must be at least 0.375 to achieve the required blade metal temperature of 1250°C. These cooling hole configurations served as the foundation for developing an RSM-based predictive model, which predicts $T_{m,\max}$ and guides design modifications to maintain blade metal temperatures below 1250°C.

2.2 | Design of Experiment (DOE)

The BBD utilized the DOE to identify the design points necessary for analyzing the impact of cooling hole configurations on $T_{m,\max}$ at the blade's LE. A set of structured simulation runs was created based on three carefully chosen independent

TABLE 3 | The levels of independent variables.

Variables, unit	Symbol	Levels		
		+1	0	1
Blade height (H), mm	A	300	188	76
Hole diameter (d), mm	B	4.8	3.4	2.0
Spacing between holes (s_x), mm	C	7.0	4.75	2.5

variables. BBD is selected due to its ability to fit a second-order (quadratic) model using a combination of factor levels. $T_{m,\max}$ was defined as the objective function for the optimization. The effect of different geometrical factors on the cooling performance was investigated using a three-level, three-continuous factor design. The list of the independent variables (A, B, and C) with their codes and actual levels is presented in Table 3. The factor variables were studied and varied across three levels: a high level, represented as (+1); a low level, represented as (0); and a middle point, expressed as (0). A second-order polynomial equation was chosen to fit the results. This model represents the main effects of the independent variables (A, B, and C) and their interactions on the response variable, y, which is $T_{m,\max}$.

2.3 | RSM to Obtain Optimal Cooling Hole Configuration

RSM establishes the relationship between the input variables (H, d, and s_x) and the response variable, the $T_{m,\max}$. RSM models the response surface, which is a mathematical representation of the metal temperature based on the input variables. This surface will serve as the basis for optimizing the cooling hole configuration. A regression model is developed that relates the design variables (cooling hole configurations) to the output performance metrics ($T_{m,\max}$). The model's accuracy is assessed using statistical metrics, such as the R-squared value (which should be as close to 1 as possible) and the p value (which should be less than 0.05), ensuring that the model accurately represents the relationships between the design variables and the objective. The developed regression model is validated through a fit test using ANOVA. Minitab software is used to generate a candidate design set for further analysis. Response optimizer is used to determine the suggested optimal value for each continuous factor based on the set target $T_{m,\max}$, which is below 1250°C.

2.4 | Thermal Analysis From FSI

A comprehensive CHT analysis was conducted using SolidWorks Flow Simulation to investigate the thermal behavior of turbine blades under realistic operating conditions of the advanced GT. The study integrates FSI modeling to capture the coupled effects of conduction through solid materials and convection from hot gases, as well as internal cooling air. The computational model consisted of three domains: a solid domain representing the Inconel 738LC superalloy blade with TBC, a fluid domain simulating the interaction between mainstream hot gas at 1400°C and coolant air at 400°C, and a solid–fluid interface resolving the thermal exchange across conduction and convection boundaries.

While both cylindrical and shaped holes are widely employed in film cooling designs, this study focuses exclusively on cylindrical holes due to a combination of practical, structural, and manufacturability considerations. Cylindrical holes are simpler to fabricate, offer robust mechanical integrity, and are more cost-effective for large-scale turbine applications [23, 24]. Although shaped holes, with diffusing outlets, can enhance film spread and lateral cooling [25, 26], they also introduce manufacturing complexity, increased cost, and flow instabilities, particularly near the blade LE [19, 27]. Additionally, shaped or oval holes have been associated with debris ingestion, oxidation, and pitting damage during operation due to their wider openings [28]. Therefore, this study prioritizes cylindrical holes as a practical and industrially relevant baseline, particularly in high-temperature regions such as the LE, where robustness, manufacturability, and coolant stability are crucial. From Table 1, the most used injection angle is 30°.

A comprehensive modeling framework was implemented for the CHT analysis of internally cooled turbine blades using SolidWorks Flow Simulation. An actual turbine blade model, featuring hybrid cooling protection that includes both TBC and internal cooling, was used as the basis for the FSI analysis. Using SolidWorks' sketch tools, the blade's geometric profile was created by sketching cross-sections at specified positions (top, 1/4, 1/2, bottom, and hub). Each sketch accurately represented the blade's shape and dimensions at those locations along its length, incorporating specific aerofoil coordinates at 100%, 50%, and 0% span. Section curves were generated in the (x, y) plane for various blade spans, with the space between these curves corresponding to the blade's height along the z-axis. The lofted extrude tool was then used to construct the 3D geometry of the blade profile.

Geometry preparation and domain decomposition were carried out with separate domains for solid (blade, bond coat, and topcoat), fluid (hot gas and coolant), and solid–fluid interfaces. The employed flow model is illustrated in Figure 1. Mesh generation used adaptive refinement, particularly near high-gradient regions such as cooling holes, the LE, and material interfaces. SolidWorks Flow Simulation solves the

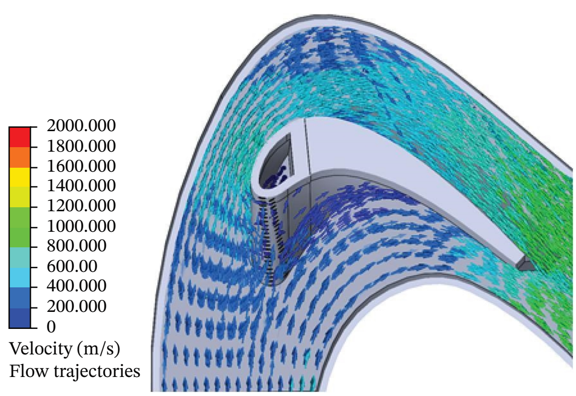

FIGURE 1 | The blade flow simulation model.

fundamental equations of CFD using the governing equations based on the fundamental laws of conservation: mass, momentum, and energy, which are represented by the continuity equation, the Navier–Stokes equations, and the energy equation, defined, respectively, as

Mass (continuity equation):

$$\frac{\delta \rho}{\delta t}+\frac{\delta(\rho u_i)}{\delta x_i}=0,$$

Momentum (Navier–Stokes):

$$\frac{\delta(\rho u_i)}{\delta t}+\frac{\delta}{\delta x_j}(\rho u_i u_j)+\frac{\delta P}{\delta x_i}=\frac{\delta}{\delta x_j}\left(\tau_{ij}+\tau_{ij}^R\right)+S_i,$$

Energy conservation:

$$\frac{\delta \rho H}{\delta t}+\frac{\delta \rho u_i H}{\delta x_i}=\frac{\delta}{\delta x_i}\left(u_j\left(\tau_{ij}+t_{ij}^R\right)+q_i\right)+\frac{\delta p}{\delta t}-\tau_{ij}^R\frac{\delta u_i}{\delta x_j}+\rho\epsilon+S_i u_i+Q_H.$$

Heat transfer interactions across solid–fluid interfaces are resolved by enforcing continuity of thermal flux:

$$\frac{\delta \rho e}{\delta t}=\frac{\delta}{\delta x_i}\left(\lambda_i\frac{\delta T}{\delta x_i}\right)+Q_H.$$

Basic simulation settings were established, including steady-state conditions, a blowing ratio of 1.0, coolant and mainstream pressures of 17 MPa, and inlet temperatures of 400°C (coolant) and 1400°C (mainstream). Convergence criteria were set to residuals less than 1×10^{-4} for continuity and less than 1×10^{-5} for energy. This simulation accounts for heat transfer between the turbine inlet hot gas and the blade, the effectiveness of the TBC layer, and the impact of the internal and external cooling provided by the holes. The thermal load is modeled accurately to simulate real GT operating conditions. The simulations provide detailed information on the temperature distribution across the blade's most critical region, the LE.

The TBC comprises a conventional yttria-stabilized zirconia (YSZ) topcoat layer, NiCrAlY bond coat layer, and In738 Ni-based superalloy blade material. The material properties are listed in Table 4.

2.5 | Model Validation Methodology

Residual analysis was conducted to verify the adequacy of the regression model. Specifically, residuals, which are the differences between observed (or simulated) and model-predicted responses, were analyzed for normality, constant variance,

TABLE 4 | Thermal properties used.

Material	Material thermal conductivity, W/(m·K)	Mass density, kg/m³	Specific heat, J/kg·K
YSZ topcoat	2.40 [29]	3610 [30]	505 [30]
NiCrAlY bond coat	16.10 [31]	7380 [31]	450 [31]
In738 superalloy	14.30 [32]	4430 [33]	526.3 [33]

and independence. A normal probability plot of residuals was constructed to assess the distribution characteristics of the errors. Points aligning along a straight line in this plot would indicate a normal distribution of residuals, a critical assumption underpinning the validity of RSM. Additionally, residual plots against predicted values were examined to detect potential patterns that can lead to inaccurate and misleading results.

3 | Results and Discussions

3.1 | Optimization of Cooling Hole Configuration for Turbine Blade Thermal Management

3.1.1 | Parametric Analysis and RSM

The FSI simulations yielded $T_{m,\max}$ values for each cooling hole configuration, which were used to develop response surfaces via ANOVA (see Table 5) and generate a regression equation from the responses (Equation (3)). The developed equation was quantified via ANOVA (Table 5). Notably, the interaction term BC (hole diameter × spacing) was highly significant ($p < 0.01$), reinforcing the coupled nature of these variables in governing cooling effectiveness. The regression model effectively captured the nonlinear relationship between design variables and $T_{m,\max}$, with an R^2 of 98.36%, indicating that the model accurately fits the FSI simulation results. The valid ranges for the parameters in Equation (3) correspond directly to the low, middle, and high levels of the independent variables used in the RSM design (see Table 4). Table 6 presents the simulation and RSM-predicted $T_{m,\max}$ values, demonstrating prediction errors within acceptable limits (< 10%). This highlighted the need for balanced design trade-offs:

$$\begin{aligned}T_{m,\max}&=1284-0.452H-32.3d\\&+12.9s_x-0.00025H^2+6.21d^2-0.5{s_x}^2\\&+0.018Hd+0.0718Hs_x-0.01ds_x.\end{aligned}\tag{3}$$

3.1.2 | Influence of Individual and Interaction Effects

This study examines the impact of structural parameters on the temperature of blade metal under high thermal loads. These parameters were chosen based on their demonstrated impact on cooling effectiveness in prior GT research, practical relevance in real-world blade designs, and manufacturability considerations.

TABLE 5 | Results of statistical analysis—ANOVA table.

Source	*df*	Sum of squares	Mean square	*F* -value	*p* value
Model	9	10,673.0	1185.89	1.74	0.028
A—blade height, *h* (mm)	1	24.5	24.50	0.04	0.085
B—diameter, *d* (mm)	1	1891.1	1891.13	2.78	0.015
C—spacing, s_x (mm)	1	2346.1	2346.13	3.45	0.012
A^2	1	685.4	685.44	1.01	0.036
B^2	1	685.4	685.44	1.01	0.036
C^2	1	1082.8	1082.83	1.59	0.026
AB	1	0	0	0	0.1
AC	1	49.0	49.00	0.07	0.065
BC	1	3782.2	3782.25	5.56	0.006
Lack of fit	3	3400.7	1133.58		
Pure error	2	0	0		
Total	14	14,073.7			

A critical literature survey reveals that hole diameters in practical GT blades commonly range from 2.0 to 4.8 mm, with blade heights from 76 to 300 mm across different designs. Most experimental and computational studies focus on optimizing hole size and distribution rather than complex hole geometries, which are often limited by manufacturing tolerances and cost. The impact and interactions of each parameter were quantified using a three-factor, three-level complete factorial design, analyzed via RSM. Figure 2 presents the resulting 3D surface plots, which show the effects of H, d, and s_x on $T_{m,\max}$.

Figure 2a shows a concave response surface for $H \times d$. The lowest $T_{m,\max}$ values occur at intermediate diameters; the interaction between blade height and hole diameter indicates that the most extended blade height (300 mm) with small (around 2 mm) or large (around 4.8 mm) diameters is a good combination for reducing $T_{m,\max}$.

Figure 2b shows the impact of spacing between holes on thermal performance. This plot shows similar agreement with the above discussion that the most extended blade (300 mm) can reduce the $T_{m,\max}$, with intermediate spacing to below. This configuration might enable both adequate film development along the blade surface and optimal lateral coverage between adjacent cooling holes. The smaller spacing seems to encourage continuous film coverage, reducing hot spots and promoting a more uniform thermal boundary.

Figure 2c illustrates the concave region where optimal cooling occurs at large hole diameters and small spacing. Larger

TABLE 6 | Regression statistics.

No.	Variable			Response		
	A	*B*	*C*	From FSI simulation	From the RSM prediction	Error %
1	76	2	2.5	1390	1253.9	9.8
2	76	2	4.75	1400	1287.0	8.1
3	76	3.4	4.75	1400	1290.6	7.8
4	76	3.4	7	1400	1318.6	5.8
5	76	4.8	2.5	1400	1285.5	8.2
6	188	2	7	1376	1317.3	4.3
7	188	2	4.75	1400	1271.2	9.2
8	188	2	4.75	1400	1271.2	9.2
9	188	3.4	4.75	1400	1277.6	8.7
10	188	4.8	4.75	1340	1308.4	2.4
11	188	4.8	7	1383	1354.4	2.1
12	300	2	7	1400	1313.4	6.2
13	300	3.4	4.75	1371	1258.4	8.2
14	300	3.4	7	1385	1322.6	4.5
15	300	4.8	7	1400	1356.1	3.1

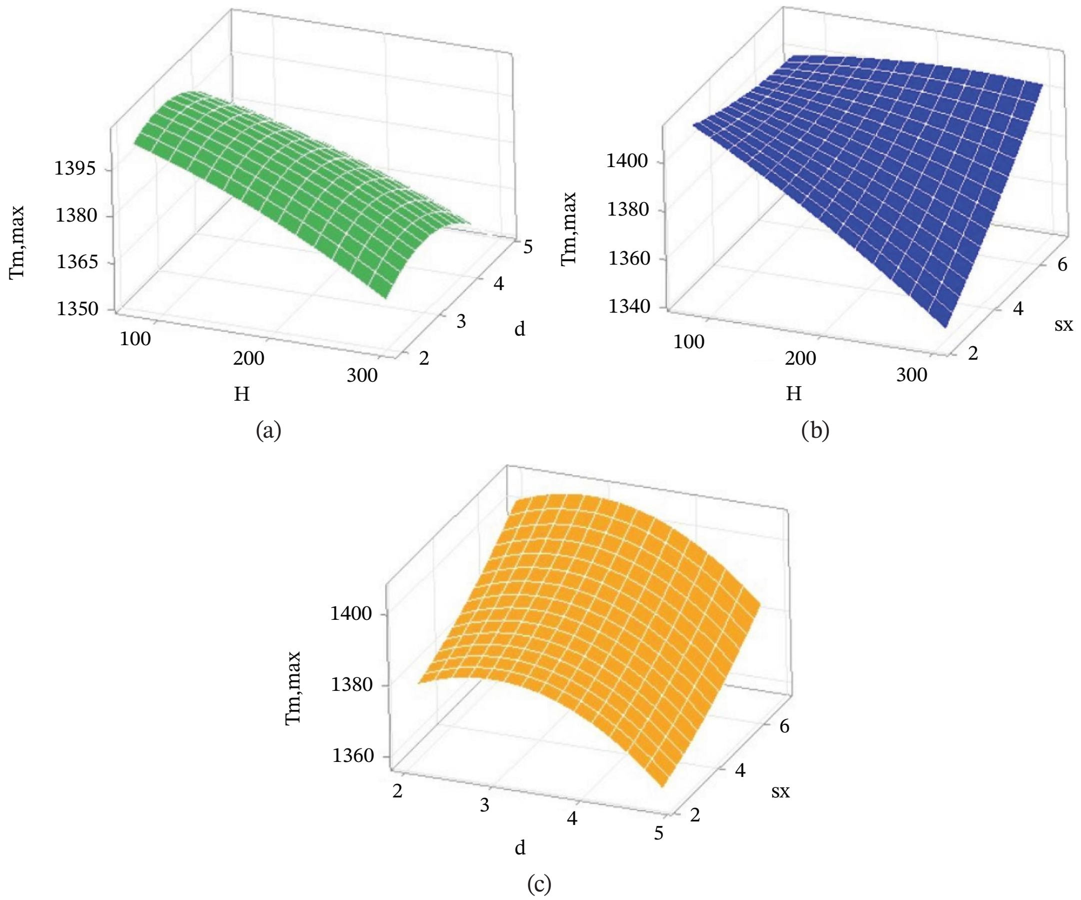

FIGURE 2 | Surface plot for continuous factors between (a) blade height, H, and cooling hole diameter, d; (b) blade height, H, and spacing between holes, s_x; and (c) cooling hole diameter, d, and spacing between holes, s_x.

diameters increase the flow rate but can cause detachment of the cooling film, thereby decreasing film adhesion near the LE, which is consistent with the findings of Bai et al. [33] and Yang et al. [34]. In contrast, excessively narrow spacing might lead to coolant merging and turbulent interactions, diminishing film stability. These findings align with observations by Liu et al. [35], who reported that overly tight hole configurations disrupt smooth film development, while properly spaced holes allow for better lateral coverage and adherence.

Applying the RSM equation to real-world turbine blade configurations necessitates careful consideration of geometric and operational constraints, as these factors directly impact cooling effectiveness, structural integrity, manufacturability, and long-term durability in high-temperature environments. Blade height, for instance, is inherently limited by aerodynamic stage requirements and mechanical load-bearing capacity. Although this study considered heights ranging from 76 to 300 mm, industrial applications typically use blade heights above 150 mm, depending on the turbine's pressure stage and classification [36, 37]. While taller blades offer a larger surface area for cooling, they must be designed within mechanical limits to avoid issues such as excessive centrifugal stress and vibration [38]. Hole diameter must strike a balance between efficient coolant discharge, structural integrity, and manufacturability. Diameters below 2 mm are prone to clogging and present fabrication challenges, while larger diameters may cause film lift-off, reducing adhesion and local cooling performance [39, 40]. Spacing between holes is constrained by the curvature

TABLE 7 | The proposed cooling hole configuration.

Parameter	Value
Blade height (H), mm	300
Cooling hole diameter (d), mm	2.0
Spacing between holes (s_x), mm	4.75
Number of cooling holes (n)	45

and limited surface area near the blade's LE. Too-narrow spacing can cause coolant streams to interfere and become turbulent, particularly with shaped holes, whereas overly wide spacing allows hot gases to infiltrate between streams, undermining thermal protection [39, 41].

The response optimizer in Minitab identified an optimal configuration consisting of a 300 mm blade height, a 2.0 mm hole diameter, and a 4.75 mm spacing, which requires a total of 45 cooling holes, as determined using Equation (2), as detailed in Table 7.

3.2 | Thermal Performance Evaluation of Cooling Configurations

Figure 3 presents temperature contours across the blade surface, further illustrating how cooling hole configurations influence

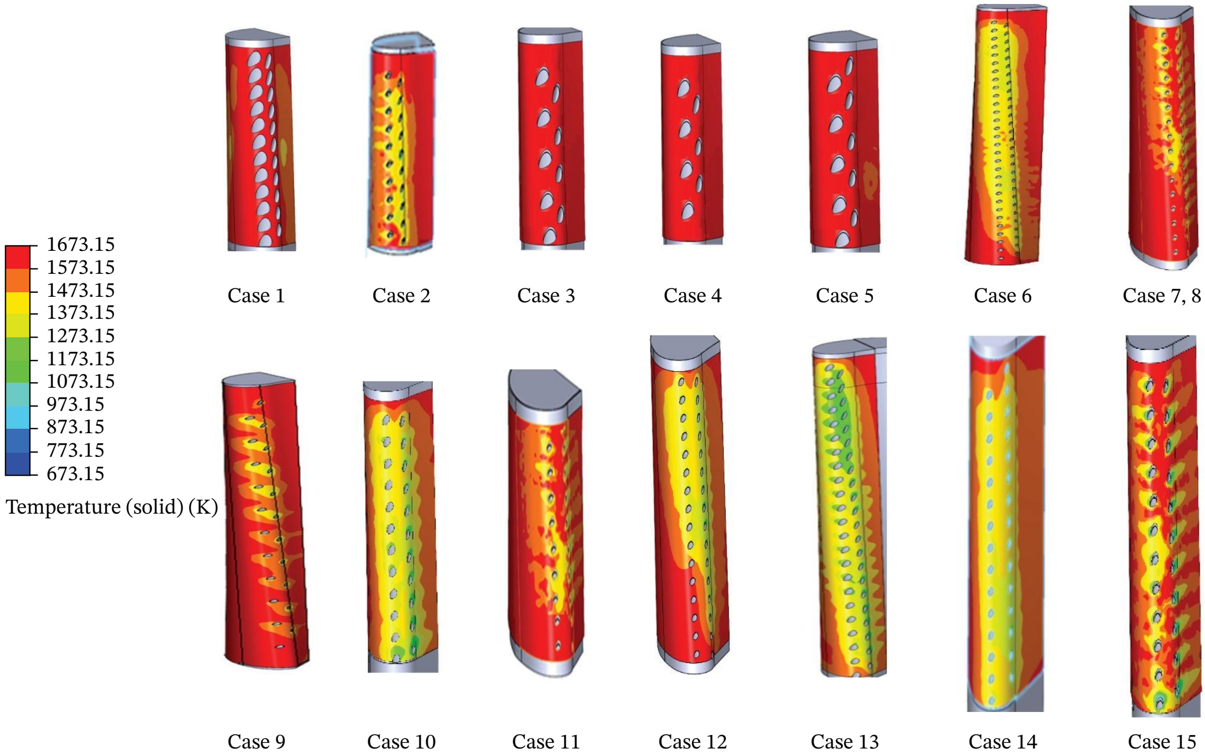

FIGURE 3 | Temperature profile of the Ni-based metal substrate for all the cooling hole configurations.

temperature distribution, particularly at the minimum blade height. At 76 mm, all configurations show limited cooling effectiveness, regardless of hole size or spacing. For instance, Case 1, featuring the smallest diameter (2.0 mm) and closest spacing (2.5 mm), shows significant thermal accumulation due to restricted coolant flow and poor surface coverage. Increasing hole diameter in Cases 3 and 5 (3.4 and 4.8 mm, respectively) does not significantly improve cooling, suggesting that at this low blade height, the coolant film lacks space to form and develop effectively. This indicates that thermal conduction from the hot mainstream gas dominates the blade surface temperature, rendering variations in diameter or spacing relatively ineffective at this scale.

In contrast, Cases 6 through 8, all with a constant 2.0 mm diameter but varying spacing (7.0 and 4.75 mm), isolate the effect of spacing. Increased spacing improves cooling continuity along the axial direction but may compromise localized intensity. Cases 9–11, which utilize larger hole diameters (3.4 and 4.8 mm), demonstrate better temperature uniformity, especially in the upper blade regions, underscoring the combined importance of adequate blade height and hole diameter for effective thermal control. These results align with Sharma et al. [42], who emphasized the need for consistent film formation to reduce hotspots. Larger hole diameters also enhance coolant flow trajectory and reduce the risk of clogging from particulates, consistent with the findings of Zhou et al. [43] and Xu et al. [44]. However, Case 11 reveals that excessively wide spacing cannot fully compensate for the lack of targeted cooling, highlighting the importance of balancing spacing with diameter and height to achieve optimal thermal performance.

The increased blade height enables the development of a fully formed coolant film, which, when combined with optimized hole diameter and spacing, ensures broader and more effective surface coverage. Even with moderately spaced holes, as seen in Case 13 ($s_x = 4.75$ mm), the temperature distribution remains well controlled, underscoring the stabilizing effect of extended axial length on thermal diffusion. However, prominent hotspots at the blade tip were observed for these tallest blade height configurations, with $T_{m,\max}$ approaching 1400°C. This is attributed to inadequate cooling coverage resulting from coolant lift-off and poor film formation in critical regions, consistent with the findings of Cunliang et al. [45] and Zhou et al. [43]. Coolant detachment, often intensified by steep velocity gradients, leads to localized thermal stress, increasing the risk of material degradation. Additionally, the formation of counter-rotating vortex pairs (CRVPs) further destabilizes the cooling film. These structures, generated by interactions between the coolant stream and the mainstream hot gases, disrupt film continuity: a phenomenon also described by Zhu et al. [30] in their analysis of film cooling instabilities.

Based on the optimized cooling hole configuration detailed in Table 7, the holes were positioned accordingly, as shown in Figure 4. Figure 4c illustrates the metal temperature distribution achieved using the proposed cooling hole configuration. This optimized arrangement effectively reduced the $T_{m,\max}$ to 1210°C, significantly improving the thermal profile and bringing the maximum temperature well below the critical operational threshold of 1250°C, thereby confirming the configuration's effectiveness. The resulting temperature contours demonstrate uniform cooling with minimal thermal gradients across the blade surface. Additionally, the regression model (Equation 3) predicts a $T_{m,\max}$ of 1249.75°C, which aligns with the target set at the outset of the RSM analysis, further validating the optimization approach.

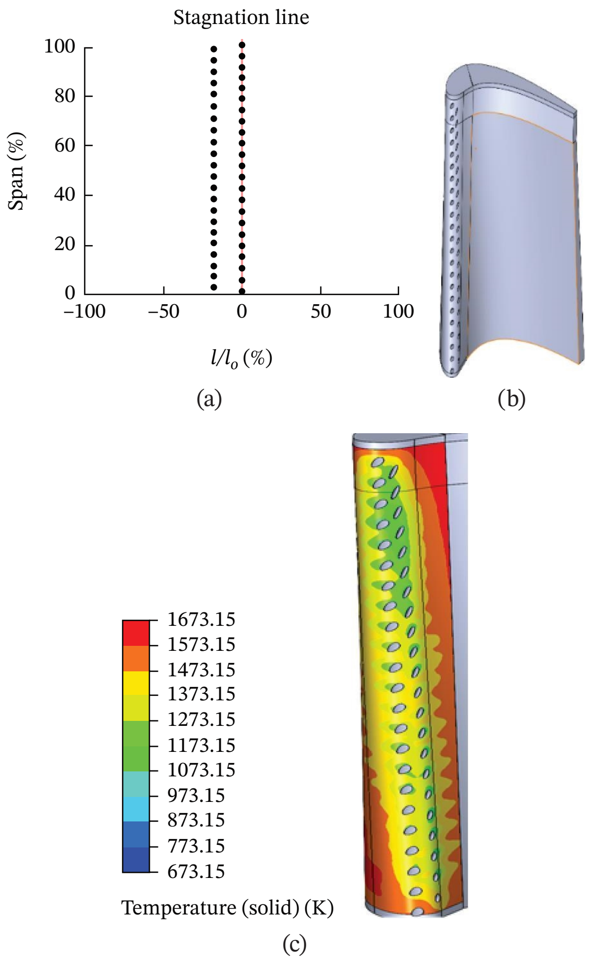

FIGURE 4 | (a) The new cooling hole configuration, (b) the 3D model, and (c) the contour of the blade metal temperature.

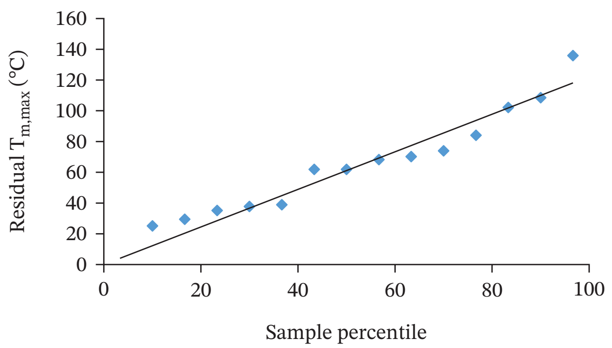

FIGURE 5 | A normal probability plot of residuals.

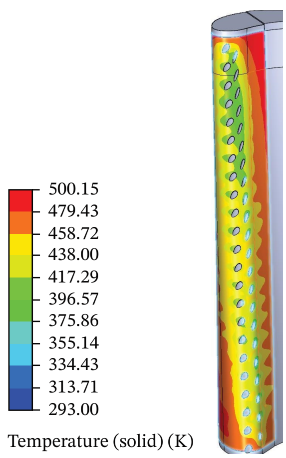

FIGURE 6 | Temperature distribution from using parameters from Islami et al. [26].

3.3 | Validation of the Optimized Cooling Design

The regression model developed through RSM exhibited a high coefficient of determination ($R^2 = 98.36\%$), indicating strong explanatory power for the observed data. The adjusted R^2 (91.89%) further corroborated the model's reliability after accounting for the number of predictors. A normal probability plot of residuals was constructed (see Figure 5). It was found that the normal probability plot of residuals exhibited a near-linear trend, with only minor deviations at the extremes, confirming that the errors were approximately normally distributed. This observation validates one of the core assumptions of the RSM model, reinforcing the reliability of statistical inference drawn from the model. Moreover, the normality of residuals supports the appropriateness of using a parametric method, such as ANOVA, to assess the influence of design variables on the response ($T_{m,\max}$). This further substantiates the model's adequacy in capturing the underlying physics of turbine blade thermal behavior within the studied parameter space.

3.4 | Validation of the Model

The developed LE cooling model was validated by replicating a benchmark case from Islami et al. [26], as illustrated in Figure 6. The validation process involved reproducing identical geometric, boundary, and thermal conditions reported in the reference study to ensure consistency in flow and heat transfer characteristics. The $T_{m,\max}$ obtained from the present simulation was 209°C, closely matching the benchmark value of 214.6°C, with a deviation of only 2.6%. This minor discrepancy confirms that the developed model can accurately predict the CHT and thermal response of turbine blade LE regions, thereby ensuring its reliability for further optimization of cooling hole configurations under real turbine operating conditions.

4 | Conclusion

In the open literature, numerous studies focus on turbine blade external heat transfer, film cooling, and the crucial parameter of cooling effectiveness. To meet the higher TIT of advanced GT, a hybrid turbine blade protection system incorporating TBC and an advanced cooling system is essential for the next generation of turbine blade designs. Additionally, highly accurate and detailed local heat transfer data are required in critical turbine edge regions to ensure that advanced turbine blade cooling provides maximum coverage, effectively protecting the substrate surface. An RSM analysis was performed to optimize the cooling hole configuration. The study identified that the optimal cooling hole configuration for a 300 mm blade height consists of 45 holes, each with a diameter of 2.0 mm, arranged in a staggered pattern with a spacing of 4.75 mm between the holes. A subsequent FSI simulation revealed a $T_{m,\max}$ of 1210°C, which is within the required limit of 1250°C. The established regression model predicts a $T_{m,\max}$ of 1249.75°C, closely matching the target established at the beginning of the RSM analysis, thereby reinforcing the validity and reliability of the optimization strategy. An improved cooling hole configuration for advanced GT blades transforms turbine performance. Enhanced cooling designs not only extend the durability of the blades by mitigating thermal stresses and preventing premature material degradation, but they also offer significant cost savings in maintenance and replacement. Furthermore, optimized cooling enables turbines to operate at higher temperatures, boosting overall efficiency and enhancing operational flexibility.

Acknowledgments

The authors acknowledge TNB Research Sdn Bhd, Universiti Tenaga Nasional, and UNITEN R&D Sdn Bhd. Special thanks are due to those who contributed directly or indirectly to this project.

Funding

No funding was received for this manuscript, but both organizations, TNB Research Sdn Bhd and Universiti Tenaga Nasional, have supported it in terms of facilities and supervision.

Conflicts of Interest

The authors declare no conflicts of interest.

Data Availability Statement

The authors confirm that the data supporting the findings of this study are available within the article.

References

1. W. Du, L. Luo, Y. Jiao, S. Wang, X. Li, and B. Sunden, "Heat Transfer in the Trailing Region of Gas Turbines–A State-of-the-Art Review," *Applied Thermal Engineering* 199 (2021): 117614, https://doi.org/10.1016/j.applthermaleng.2021.117614.

2. J. C. Han, "Advanced Cooling in Gas Turbines 2016 Max Jakob Memorial Award Paper," *Journal of Heat Transfer* 140, no. 11 (2018): 113001, https://doi.org/10.1115/1.4039644.

3. K. Takamura, T. Iijima, S. Wakazono, S. Hada, M. Yuri, and M. Kataoka, "Development of 1650° C Class Next Generation JAC Gas Turbine Based on J Experience," *Mitsubishi Heavy Industries Technical Review* 56, no. 3 (2019): 1.

4. H. W. Li, F. Han, H. C. Wang, Z. Y. Zhou, and Z. Tao, "Film Cooling Characteristics on the Leading Edge of a Rotating Turbine Blade With Various Mainstream Reynolds Numbers and Coolant Densities," *International Journal of Heat and Mass Transfer* 127 (2018): 833–846, https://doi.org/10.1016/j.ijheatmasstransfer.2018.07.126.

5. L. Shi, Z. Sun, and Y. Lu, "The Combined Influences of Film Cooling and Thermal Barrier Coatings on the Cooling Performances of a Film and Internal Cooled Vane," *Coatings* 10, no. 9 (2020): 861, https://doi.org/10.3390/coatings10090861.

6. R. Abdelmaksoud, and T. Wang, "Simulation of Air/Mist Cooling in a Conjugate, 3-D Gas Turbine Vane With Internal Passage and External Film Cooling," *International Journal of Heat and Mass Transfer* 160 (2020): 120197, https://doi.org/10.1016/j.ijheatmasstransfer.2020.120197.

7. H. Du, Z. Mei, J. Zou, W. Jiang, and D. Xie, "Conjugate Heat Transfer Investigation on Swirl-Film Cooling at the Leading Edge of a Gas Turbine Vane," *Entropy* 21, no. 10 (2019): 1007, https://doi.org/10.3390/e21101007.

8. A. Singh, A. K. Pujari, and B. V. S. S. S. Prasad, "Conjugate Heat Transfer Analysis of a Rotor Blade With Coolant Channels," *Heat Transfer* 50, no. 7 (2021): 6816–6846, https://doi.org/10.1002/htj.22205.

9. Z. Jiang, Z. Liang, L. Zhu, Z. Guo, and Y. Tang, "Effect of Hole Diameter of Rotary-Shaped Artificial Reef on Flow Field," *Ocean Engineering* 197 (2020): 106917, https://doi.org/10.1016/j.oceaneng.2020.106917.

10. B. Zhang, Y. X. Chen, Z. G. Wang, J. Q. Li, and H. H. Ji, "Influence of Mach Number of Main Flow on Film Cooling Characteristics Under Supersonic Condition," *Symmetry* 13, no. 1 (2021): 127, https://doi.org/10.3390/sym13010127.

11. J. H. Liu, Y. B. Liu, and L. Liu, "Film Cooling Modeling of a Turbine Vane With Multiple Configurations of Holes," *Case Studies in Thermal Engineering* 11 (2018): 71–80, https://doi.org/10.1016/j.csite.2018.01.001.

12. M. Kim, D. H. Shin, B. J. Lee, and J. Lee, "Experimental and Numerical Investigation of Micro-Scale Effusion and Transpiration Air Cooling on Cascaded Turbine Blades," *Case Studies in Thermal Engineering* 32 (2022): 101892, https://doi.org/10.1016/j.csite.2022.101892.

13. L. Shi, Y. Lu, and H. Huang, "Analysis of Rotor–Stator Interaction on the Aerothermal and TBC Insulation Performance of a Turbine Stage Under Hot Streak Inlet Condition," *Coatings* 12, no. 1 (2022): 25, https://doi.org/10.3390/coatings12010025.

14. X. D. Zhang, J. J. Liu, and C. Li, "A Cooled Turbine Airfoil Performance Prediction Method With Two-Dimensional CFD Computation and Loss Models," *International Journal of Turbo & Jet-Engines* 41, no. 1 (2024): 71–80, https://doi.org/10.1515/tjj-2022-0044.

15. F. Wen, R. Hou, Y. Luo, and S. Wang, "Study on Leading-Edge Trenched Holes Arrangement Under Real Turbine Flow Conditions," *Engineering Applications of Computational Fluid Mechanics* 15, no. 1 (2021): 781–797, https://doi.org/10.1080/19942060.2021.1919211.

16. X. Huang, J. Pu, J. H. Wang, Y. F. Qu, and J. H. He, "Sensitivity Analysis of Internal Layout and Coating Thickness to Overall Cooling Performances of Laminated Cooling Configurations With Surface Thermal Barrier Coatings," *Applied Thermal Engineering* 181 (2020): 116020, https://doi.org/10.1016/j.applthermaleng.2020.116020.

17. M. Effendy, Y. F. Yao, J. Yao, and D. R. Marchant, "Detached Eddy Simulation of Blade Trailing-Edge Cutback Cooling Performance at Various Ejection Slot Angles," *International Journal of Heat and Fluid Flow* 80 (2019): 108487, https://doi.org/10.1016/j.ijheatfluidflow.2019.108487.

18. J. Wang, C. Liu, Z. Zhao, J. Baleta, and B. Sundén, "Effect and Optimization of Backward Hole Parameters on Film Cooling Performance by Taguchi Method," *Energy Conversion and Management* 214 (2020): 112809, https://doi.org/10.1016/j.enconman.2020.112809.

19. M. Zhang, N. Wang, and J. C. Han, "Overall Effectiveness of Film-Cooled Leading Edge Model With Normal and Tangential Impinging Jets," *International Journal of Heat and Mass Transfer* 139 (2019): 577–587, https://doi.org/10.1016/j.ijheatmasstransfer.2019.05.037.

20. L. Cai, Y. He, S. Wang, Y. Li, and F. Li, "Thermal-Fluid-Solid Coupling Analysis on the Temperature and Thermal Stress Field of a Nickel-Base Superalloy Turbine Blade," *Materials* 14, no. 12 (2021): 3315, https://doi.org/10.3390/ma14123315.

21. V. G. Krishna Anand, and K. M. Parammasivam, "Thermal Barrier Coated Surface Modifications for Gas Turbine Film Cooling: A Review," *Journal of Thermal Analysis and Calorimetry* 146, no. 2 (2021): 545–580, https://doi.org/10.1007/s10973-020-10032-2.

22. R. Yu, H. Han, C. Yang, and W. Luo, "Optimal Design and Decision Making of an Air Cooling Channel With Hybrid Ribs Based on RSM and NSGA-II," *Journal of Thermal Analysis and Calorimetry* 147, no. 10 (2022): 5839–5854, https://doi.org/10.1007/s10973-021-10807-1.

23. V. Prakash, S. Chandel, D. G. Thakur, M. P. Mishra, and R. K. Mishra, "Effect of Multi-Hole Arrangement on the Effusion Cooling With Backward Injection," *International Journal of Turbo & Jet-Engines* 40, no. 4 (2023): 387–397, https://doi.org/10.1515/tjj-2021-0023.

24. R. Zhu, T. W. Simon, and G. Xie, "Influence of Secondary Hole Injection Angle on Enhancement of Film Cooling Effectiveness With Horn-Shaped or Cylindrical Primary Holes," *Numerical Heat Transfer, Part A: Applications* 74, no. 5 (2018): 1207–1227, https://doi.org/10.1080/10407782.2018.1490088.

25. M. Prakash Mishra, A. K. Sahani, S. Chandel, and R. K. Mishra, "Enhancement of Full Coverage Film Cooling Effectiveness With Mixed Injection Holes," *International Journal of Turbo & Jet-Engines* 39, no. 2 (2022): 205–214.

26. S. B. Islami, S. A. Tabrizi, B. A. Jubran, and E. Esmaeilzadeh, "Influence of Trenched Shaped Holes on Turbine Blade Leading Edge Film Cooling," *Heat Transfer Engineering* 31, no. 10 (2010): 889–906, https://doi.org/10.1080/01457630903550317.

27. H. W. Li, D. W. Zhang, F. Han, H. Guo, and X. F. Ding, "Experimental Investigation on the Effect of Hole Diameter on the Leading Edge Region Film Cooling of a Twist Turbine Blade Under Rotation Conditions," *Applied Thermal Engineering* 184 (2021): 116386, https://doi.org/10.1016/j.applthermaleng.2020.116386.

28. K. Sabri, M. Gaceb, and M. O. Si-Chaib, "Analysis of a Directionally Solidified (DS) GTD-111 Turbine Blade Failure," *Journal of Failure Analysis and Prevention* 20, no. 4 (2020): 1162–1174, https://doi.org/10.1007/s11668-020-00920-y.

29. M. Radovic, E. Lara-Curzio, R. M. Trejo, H. Wang, and W. D. Porter, "Thermophysical Properties of YSZ and Ni-YSZ as a Function of Temperature and Porosity," *Advances in Solid Oxide Fuel Cells II: Ceramic Engineering and Science Proceedings* 27 (2006): 79–85, https://doi.org/10.1002/9780470291337.ch8.

30. W. Zhu, J. W. Wang, L. Yang, Y. C. Zhou, Y. G. Wei, and R. T. Wu, "Modeling and Simulation of the Temperature and Stress Fields in a 3D Turbine Blade Coated With Thermal Barrier Coatings," *Surface and Coatings Technology* 315 (2017): 443–453, https://doi.org/10.1016/j.surfcoat.2017.03.012.

31. A. Aabid, J. Jyothi, J. M. Zayan, and S. A. Khan, "Experimental and Numerical Investigation on Gas Turbine Blade With the Application of Thermal Barrier Coatings," *Advances in Materials Research: AMR* 8, no. 4 (2019): 275–293, https://doi.org/10.12989/amr.2019.8.4.275.

32. O. E. Efe-Ononeme, A. Ikpe, and G. O. Ariavie, "Modal Analysis of Conventional Gas Turbine Blade Materials (Udimet 500 and IN738) for Industrial Applications," *Journal of Engineering Technology and Applied Sciences* 3, no. 2 (2018): 119–133, https://doi.org/10.30931/jetas.452857.

33. N. Bai, W. Fan, J. Zhu, et al., "Experimental Investigations Into the Effusion Plate Wall Temperature of Impingement/Effusion Cooling Systems for Gas Turbine Combustors," *Aerospace Science and Technology* 132 (2023): 108052, https://doi.org/10.1016/j.ast.2022.108052.

34. X. Yang, Z. Hao, and Z. Feng, "An Experimental Study on Turbine Vane Leading-Edge Film Cooling With Deposition," *Applied Thermal Engineering* 198 (2021): 117447, https://doi.org/10.1016/j.applthermaleng.2021.117447.

35. Y. Liu, Y. Rao, and L. Yang, "Numerical Simulations of a Double-Wall Cooling With Internal Jet Impingement and External Hexagonal Arrangement of Film Cooling Holes," *International Journal of Thermal Sciences* 153 (2020): 106337, https://doi.org/10.1016/j.ijthermalsci.2020.106337.

36. R. G. Bayro-Lazcano, S. Piedra-Gonzalez, A. I. García-Moreno, D. G. Espinosa-Arbelaez, and J. A. Villada-Villalobos, "Computational and Experimental Study on Failure Mechanism of a GTD-111 First-Stage Blade of an Industrial Gas Turbine," *Metals* 13, no. 12 (2023): 1968, https://doi.org/10.3390/met13121968.

37. C. Dahal, J. K. Tharu, and H. B. Dura, "Thermo-Structural Analysis of High-Pressure Turbine Blade," *Journal of the Institute of Engineering* 15, no. 3 (2020): 78–82, https://doi.org/10.3126/jie.v15i3.32018.

38. T. S. Chowdhury, F. T. Mohsin, M. M. Tonni, M. N. H. Mita, and M. M. Ehsan, "A Critical Review on Gas Turbine Cooling Performance and Failure Analysis of Turbine Blades," *International Journal of Thermofluids* 18 (2023): 100329, https://doi.org/10.1016/j.ijft.2023.100329.

39. J. B. Chandar, L. Nagarajan, and M. S. Kumar, "Recent Research Progress in Deep Hole Drilling Process: A Review," *Surface Review and Letters* 28, no. 11 (2021): 2130003, https://doi.org/10.1142/S0218625X21300033.

40. L. Xu, Z. Sun, Q. Ruan, L. Xi, J. Gao, and Y. Li, "Development Trend of Cooling Technology for Turbine Blades at Super-High Temperature of Above 2000 K," *Energies* 16, no. 2 (2023): 668, https://doi.org/10.3390/en16020668.

41. X. Chen, Y. Wang, Y. Long, and S. Weng, "Effect of Particle Deposition on Film Cooling From Fan-Shaped Holes," *International Journal of Heat and Mass Transfer* 181 (2021): 122028, https://doi.org/10.1016/j.ijheatmasstransfer.2021.122028.

42. C. Sharma, S. Kumar, A. Singh, et al., "Comprehensive Review on Leading Edge Turbine Blade Cooling Technologies," *International Journal of Heat & Technology* 39, no. 2 (2021): 403–416, https://doi.org/10.18280/ijht.390209.

43. J. Zhou, X. Wang, and J. Li, "Influences of Effusion Hole Diameter on Impingement/Effusion Cooling Performance at Turbine Blade Leading Edge," *International Journal of Heat and Mass Transfer* 134 (2019): 1101–1118, https://doi.org/10.1016/j.ijheatmasstransfer.2019.02.054.

44. H. Xu, K. Liu, and M. Fox, "Turbine Nozzle Insert Clogging With Seeded Medium Size Particles," in *Turbo Expo: Power for Land, Sea, and Air* 84072: (American Society of Mechanical Engineers, 2020), V02BT34A005)..

45. L. Cunliang, F. Zhang, S. Zhang, S. Qingqing, and S. Hui, "Experimental Investigation of the Full Coverage Film Cooling Effectiveness of a Turbine Blade With Shaped Holes," *Chinese Journal of Aeronautics* 35, no. 3 (2022): 297–308, https://doi.org/10.1016/j.cja.2021.06.022.